Asian Journal of Chemistry; Vol. 25, No. 9 (2013), 5181-5184

ASIAN JOURNAL OF CHEMISTRY

http://dx.doi.org/10.14233/ajchem.2013.F12

Preparation and Characterization of Flexible and Stretchable Polymeric Magnet†

U. BASULI[1], S. KIM[2], A.N. GENT[1] and C. NAH[1,2,*]

[1]Energy Harvesting WCU Research Team, Department of Polymer-Nano Science and Technology, Chonbuk National University, Jeonju, 561-756, Republic of Korea
[2]BK-21 Polymer BIN Fusion Research Team, Chonbuk National University, Jeonju 561-756, Republic of Korea

*Corresponding author: Fax: +82 63 2702341; Tel: +82 63 2704281; E-mail: cnah@jbnu.ac.kr

AJC-13168

Nano iron oxides (Fe_3O_4) with a controlled particle size were synthesized using a wet chemical method. A series of nanocomposites based on these magnetic nanoparticles and liquid silicone rubber were prepared using a direct mixing technique. A commercial grade of barium ferrite ($BaFe_{12}O_{19}$) nanoparticles with a narrow size distribution was used for the preparation of liquid silicone rubber (LSR)/$BaFe_{12}O_{19}$ nanocomposites. Transmission electron microscopy of the resulting nanocomposite (LSR/Fe_3O_4 or LSR/$BaFe_{12}O_{19}$) showed that the nanoparticles were dispersed homogeneously in the liquid silicone rubber matrix. The magnetic nanoparticles were oriented randomly in the polymeric matrix. On the other hand, when these nanocomposites were placed in a magnetic field, the nanoparticles were generally aligned along the longitudinal direction inside the matrix. The magnetic-field induced orientation of magnetic nanoparticles was observed within the polymer matrix. The super-paramagnetic property of the nanocomposite was examined by vibrating sample magnetometer analysis.

Key Words: Magnetic property, Nanocomposites, Morphology, Vibrating sample magnetometer analysis.

INTRODUCTION

Magnetism is an intrinsic material characteristic since the genesis of the Universe. Recently, magnetic nanoparticles have become a focal area of research because of their vast applications including magnetic fluids, shape memory composites, ferro fluids, catalysis, biotechnology, magnetic resonance imaging, drug delivery, biomedical applications and magnetic recording media for data storage. Many methods have been developed for their synthesis[1-3]. The defining characteristic of nanoparticles is their size. Magnetic particles show the best performance when the particle sizes are below 10-20 nm, which is smaller than the average size of a magnetic domain[4]. An assembly of nanoparticles generally consists of some distribution of sizes, approximating a log normal distribution. This distribution has a significant effect on the magnetic properties. Polymer nanocomposites are potentially important because of their many advantages over traditional polymer composites. Conventional composites normally require a high content of the filler phase to achieve the desired properties of the composite material. Nanocomposites can achieve the same properties with a much smaller amount of filler, producing materials with a lower density and higher processibility. Nanocomposites with magnetic nanoparticles dispersed in the polymer matrices have attracted considerable attention because of their wide ranging applications[5]. Below a critical size, they become a single domain in the bulk. These composites exhibit remarkable properties, such as superparamagnetism, quantum tunneling of magnetization and magnetocaloric effect [6-10].

Flexible magnets are compounds of plastics or rubber materials combined with magnetic powders of strontium ferrite and are processed by a calendaring or extrusion method to produce either sheets or coils by the roll. The finished product is a light weight, corrosion resistant, elastic and stable material that is available in rolls, sheets, tapes, strips or cut pieces, which have many practical uses, particularly in the printing and advertising industries.

Silicone is one of the most widely used polymers in insulation, coatings and rubber materials in high voltage insulation. Silicone polymers used to prepare silicone rubber compositions include inorganic and organic portions, in which each silicone chain atom has two organic groups attached to it. The properties of these materials include excellent weather and thermal stability, oxidation resistance, good electrical properties, extreme low-temperature flexibility and curability by a range of methods at both elevated and ambient temperatures[11-15].

†Presented to the International Rubber Conference (IRC-2012), May 21-24, 2012, Jeju, Republic of Korea

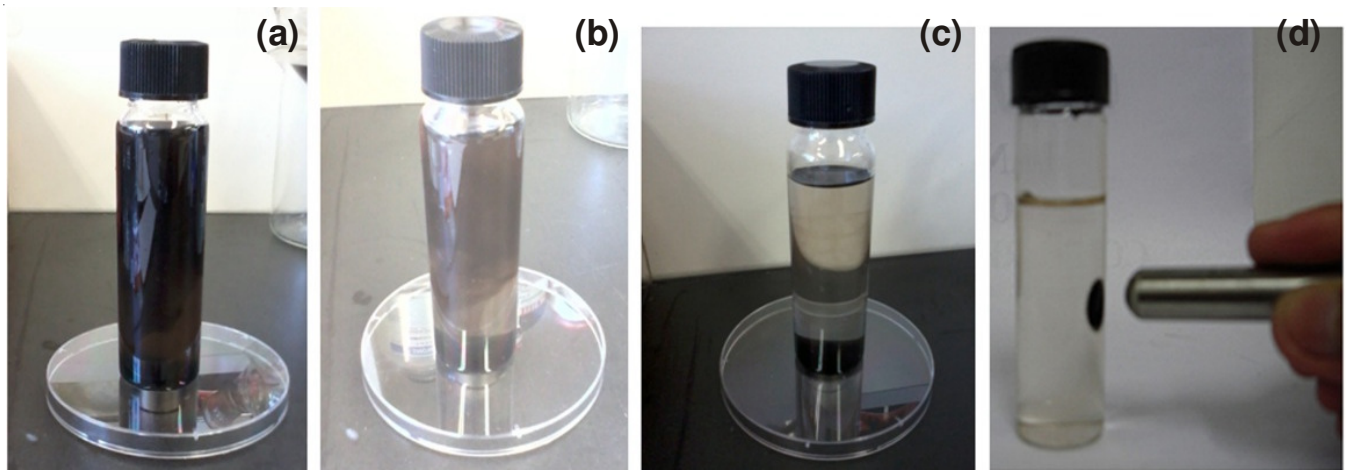

Fig. 1. Photographs of the separation and dispersion of the magnetic particles: (a) without an external magnetic field at time 0, (b) with an external magnetic field after 5 min, (c) with an external magnetic field after 15 min, (d) with an external magnetic field (the magnetic field strength of the magnet is 2000 G). The colour changes from saddle brown to transparent were observed when an external magnetic field was applied.

This paper reports the preparation of magnetic nanocomposites containing nano iron oxides (Fe_3O_4) and barium ferrite ($BaFe_{12}O_{19}$) embedded in a liquid silicone rubber (LSR) matrix. Fe_3O_4 with controlled particle size was synthesized using a wet chemical method. The nanocomposites samples were prepared using the as-prepared Fe_3O_4 and commercial barium ferrite ($BaFe_{12}O_{19}$) nanoparticles. The nanoparticles and their respective nanocomposites samples were characterized by transmission electron microscopy and vibrating sample magnetometry.

EXPERIMENTAL

Ferrous chloride hexahydrate ($FeCl_3 \cdot 6H_2O$, Sigma-Aldrich, USA, 99 %), ferric chloride tetrahydrate ($FeCl_2 \cdot 4H_2O$ Sigma-Aldrich, USA, 99 %) and concentrated NH_4OH were used as received. $BaFe_{12}O_{19}$ (dimension -325 mesh) was purchased from Sigma-Aldrich, USA, 99 %. Liquid silicone rubber (LSR) and its cross-linking agent were supplied by Sewang Hitech. Co. Ltd., Korea.

Synthesis of ferrite nanoparticles: $FeCl_3 \cdot 6H_2O$ (120 mg) was dissolved in 100 mL deionized water in a round bottom flask under N_2 atmosphere with mechanical stirring at 300 rpm at room temperature for 0.5 h. Subsequently, 180 mg of $FeCl_2 \cdot 4H_2O$ (stoichiometric ratio) was added with constant stirring in a N_2 atmosphere for 0.5 h at room temperature. A concentrated NH_4OH solution (12 mL) diluted in 60 mL of distilled water was added drop wise over a period of 1 h. At the initial stage, the colour of the solution was light yellow, which initially changed to a light wine colour after the addition of NH_4OH, then to a deep wine colour and finally to black. After several minutes, the magnetic precipitate was separated by magnetic decantation. Finally, the entire mixture was heated to 60 ºC for 2 h to remove the excess ammonia and the temperature was then increased to 85 ºC over a period of 0.5 h. At the end of the reaction, the temperature was reduced to room temperature. During the experiment, the Fe^{2+} and Fe^{3+} stoichiometric ratio was maintained to prevent the oxidation of Fe^{2+} in the system. The suspended magnetic nanoparticles were allowed to settle in an external magnetic field and separated. The precipitate was washed several times with acetone and distilled water, sequentially. The material was then washed several times with deionized water, two times with ethanol and finally evaporated to dryness to obtain Fe_3O_4 powder in a vacuum oven at 60 ºC for 24 h. Fig. 1 shows the separation technique of prepared magnetic particles. In the absence of an external magnetic field, the dispersion of magnetic particles had a saddle brown colour and was homogeneous (Fig. 1a). When the external magnetic field was applied, the magnetic particles were enriched (Fig. 1b and 1c), leading to a transparent dispersion (Fig. 1d).

Methods of preparation of nanocomposites: Magnetic nanocomposites containing magnetic nano particles, Fe_3O_4 and $BaFe_{12}O_{19}$, in a liquid silicone rubber matrix were prepared by simple mixing. Different amounts of magnetic nanoparticles (10 to 60 phr) were combined with the liquid silicone rubber. The mixer was stirred in magnetic stirrer for 2 h. Subsequently, 10 phr crosslinking agent was mixed. The mixture was stirred for a further 0.5 h to mix the crosslinker homogeneously with liquid silicone rubber. The mixes were then cast onto a glass surface. Two strong magnets were placed on the top and bottom, as depicted in Fig. 2a, at room temperature. Subsequently, the mixes were heated under vacuum at 60 ºC for 4 h (Fig. 2b) and the resulting composites sample had a mean thickness of 3 mm (Fig. 2c).

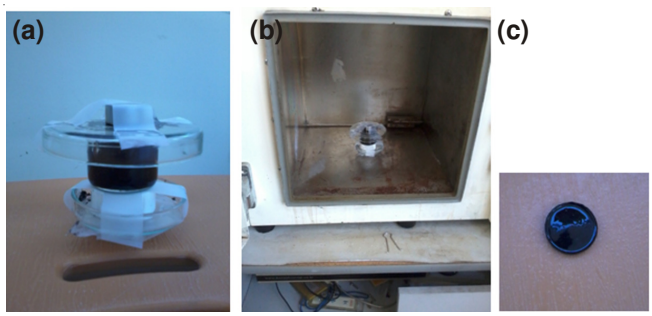

Fig. 2. Preparation of magnetic nanoparticles in liquid silicone rubber by applying an external magnetic field

Characterizations: The morphology of the superparamagnetic nanoparticles were characterized by transmission electron microscopy (TEM, H-7650, Hitachi, Japan) at an

acceleration voltage of 100 kV. One drop of an aqueous dispersion of magnetic nanoparticles was placed on a carbon coated copper TEM grid (300 mesh size) and allowed to air-dry before observation.

The morphology of various composites was examined by high-resolution TEM (HRTEM JEM 2100, JEOL, Japan) using a lanthanum hexa-boride target operating at 200 kV with a beam current of 116 μA. The samples were cut to a 50 nm thickness using Leica Ultracut EM FCS, ultracryotome, Austria. The cut samples were supported on a copper mesh before observation. A magnetic study was carried out using a vibrating sample magnetometry and SQUID magnetometer at room temperature.

RESULTS AND DISCUSSION

Morphological analysis: HRTEM clearly showed the formation of ferrite nanoparticles (Fig. 3). The mean particle size was 15-20 nm. The magnetic nanoparticles showed unique irregular morphology. The ferrite clusters were an agglomeration of nanoparticles. Interestingly, the size range is important for a broad range of applications. Selected area electron diffraction (SAED) confirmed the crystalline nature of the nanoparticles.

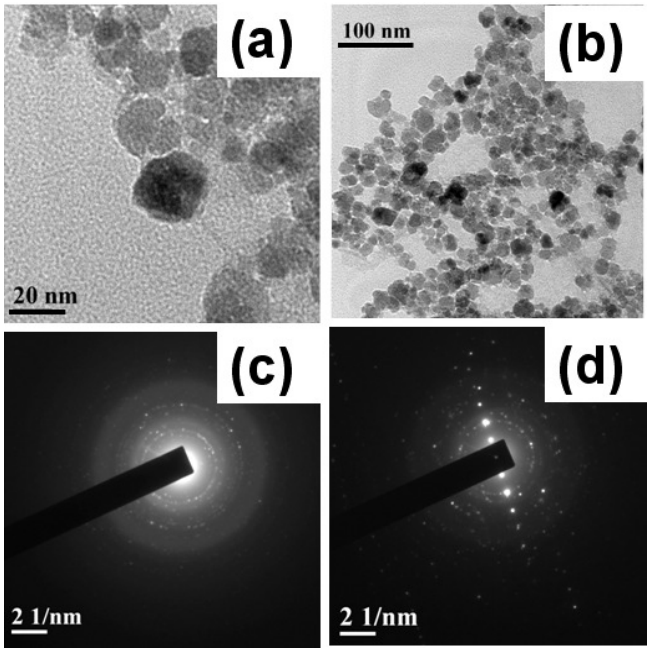

Fig. 3. HRTEM images of synthesized pristine ferrite nanoparticles and SAED patterns of ferrite nanoparticles (a) 120 k × magnification; (b) 25 k × magnification; (c) selected area diffraction of a lighter matrix obtained from a; (d) selected area diffraction of lighter matrix obtained from b

Fig. 4a-c shows TEM images of the Fe_3O_4 nanoparticles and its nanocomposites at two different magnifications, respectively. TEM clearly revealed the formation of ferrite nanoparticles. The Fe_3O_4 nanoparticles were spherical in shape and the mean particle size (diameter) was in the range of 15- 20 nm (Fig. 4a). This size range was very important for achieving strong magnetic behaviour. Fig. 3b-c shows a TEM image of the nanocomposites with 10 phr Fe_3O_4 nanoparticles. The nanoparticles were oriented in the polymer matrix. The distribution of nanoparticles was more homogeneous in the liquid silicone rubber matrix (Fig. 4b and 4c). Iron oxide nanoparticles were more dispersed in the liquid silicone rubber. Individual multi-wall nanotubes can be seen clearly. Little aggregation was observed at this loading.

Fig. 4. TEM images: (a) Ferrite Nanoparticles (b) Dispersion of 10 phr ferrite nanoparticles in liquid silicone rubber, Magnification 100 k × magnetization (c) Dispersion of 10 phr ferrite nanoparticles in liquid silicone rubber, Magnification 200 k ×

Fig. 5a-b show HRTEM images of $BaFe_{12}O_{19}$ nanoparticles and its nanocomposite containing 10 phr $BaFe_{12}O_{19}$ nanoparticles, respectively. The particles were examined by HRTEM and clusters of small $BaFe_{12}O_{19}$ particle were observed. Each individual particle was approximately 5 nm in diameter. The particles aggregated and normally precipitated during sample preparation. The magnetic nanoparticles showed a very unique irregular morphology in the liquid silicone rubber matrix. The ferrite clusters remained in an agglomerated form. TEM displays spherical particles. The barium ferrite clusters remained in an agglomerated form. Both types of particles are more aligned due to the influence of an external magnetic field.

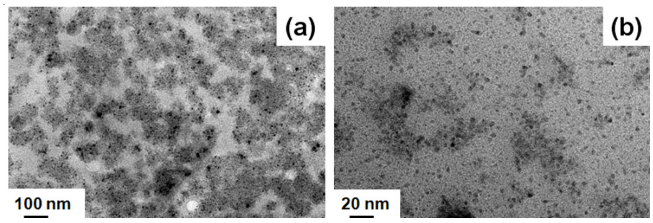

Fig. 5. HRTEM images: (a) Barium ferrite nanoparticles, Magnification 20k ×. (b) Dispersion of 10 phr barium nanoparticles in liquid silicone rubber, magnification 100k ×

Magnetic properties of nanoparticles: SQUID vibrating sample magnetometry (Fig. 6) clearly shows that the pristine ferrite nanoclusters are superparamagnetic in nature. Fig. 6 shows the hysteresis curves of the Fe_3O_4 nanoparticles and $BaFe_{12}O_{19}$ nanoparticles. The absence of a hysteresis loop indicates that thermal switching can cause spin reversal in this system. The Fe_3O_4 and $BaFe_{12}O_{19}$ nanoparticles showed superparamagnetic behaviour with saturation magnetization (Ms) values of 61.6 and 51.0 emu/g at 25 ºC, respectively.

Magnetic properties of the nanocomposites: An attempt was also made to examine the exhibition of hysteresis behaviour by these samples at room temperature. The hysteresis loop measured from vibrating sample magnetometry studies, *i.e.* Figs. 7 and 8, clearly indicates the ferromagnetic nature of the composites. The absence of a hysteresis loop indicates the superparamagnetic nature of the nanoparticles and composites (Fig. 7). The saturation magnetization was 28.8 emu/g for 10 phr Fe_3O_4 loaded composites. The data was comparable to the

data in the literature for iron oxide nanoparticle-based nanocomposites[15]. Therefore, the superparamagnetic polymer nanocomposite with different saturation magnetization values could be prepared using the Fe_3O_4 nanoparticles prepared in-house. On the other hand, the $BaFe_{12}O_{19}$ filled composites showed lower magnetization value. The presence of a hysteresis loop indicates that the nanocomposites are not superparamagnetic in nature (Fig. 8).

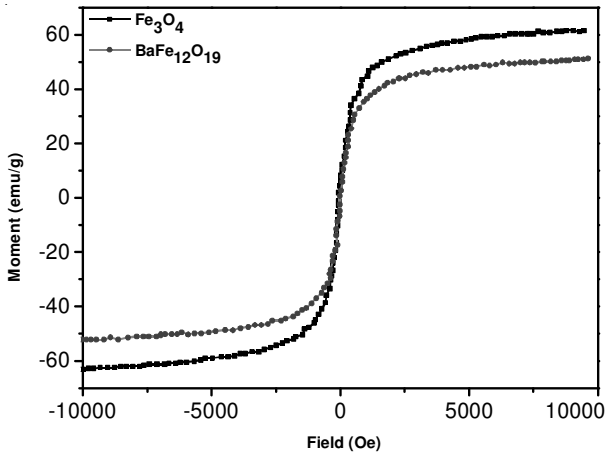

Fig. 6. Magnetization curves of the Fe_3O_4 and $BaFe_{12}O_{19}$ nanoparticles

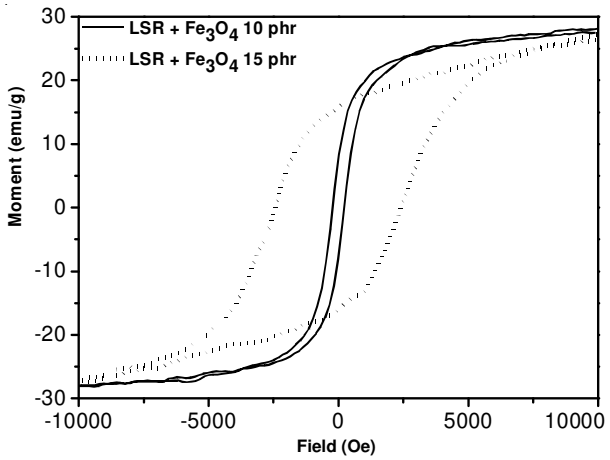

Fig. 7. Hysteresis loops (magnetization curve) of the nanocomposites containing Fe_3O_4 nanoparticles at room temperature

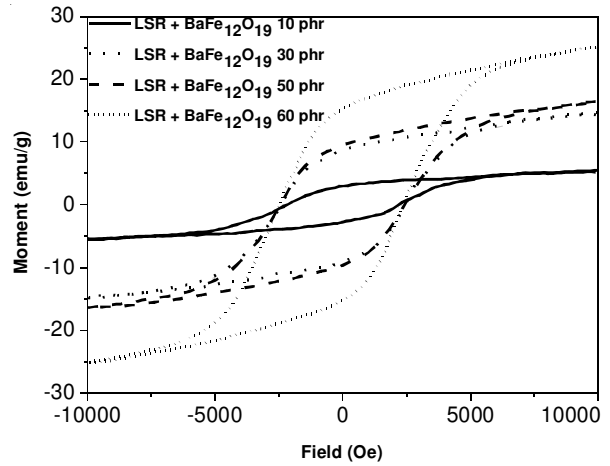

Fig. 8. Hysteresis loops (magnetization curve) of various nanocomposites containing $BaFe_{12}O_{19}$ nanoparticles at room temperature

Conclusion

Fe_3O_4 magnetic nanoparticles with a spherical shape and size (diameter) in the 15-20 nm range were synthesized for the preparation of superparamagnetic Fe_3O_4/liquid silicone rubber nanocomposites. The preparation of iron oxide nanoparticles and its nanocomposites is very simple and economical. TEM showed that the nanoparticles were well isolated, mostly with spherical shapes and only a few with faceted shapes. The nanocomposites filled with Fe_3O_4 showed superior performance than those filled with $BaFe_{12}O_{19}$ nanoparticles. The liquid silicone rubber did not affect the magnetic properties of the nanoparticles. The superparamagnetic properties of the Fe_3O_4/LSR nanocomposite were confirmed by SQUID vibrating sample magnetometry analysis.

ACKNOWLEDGEMENTS

This study was performed under the World Class University Program of the National Research Foundation of Korea, funded by the Ministry of Education, Science and Technology (R33-2008-000-10016-0).

REFERENCES

1. A.H. Lu, E.L. Salabas and F. Schüth, *Angew. Chem. Int. Ed.*, **46**, 1222 (2007).
2. D.W. Elliott and W.X. Zhang, *Environ. Sci. Technol.*, **35**, 4922 (2001).
3. M. Takafuji, S. Ide, H. Ihara and Z. Xu, *Chem. Mater.*, **16**, 1977 (2004).
4. D. Goll, A.E. Berkowitz and H.N. Bertram, *Phys. Rev. B*, **70**, 184432 (2004).
5. K.A. Malini, M.R. Anantharaman and S. Sindhu, *J. Mater. Sci.*, **36**, 821 (2001).
6. C.P. Bean and J.D. Livingstone, *J. Appl. Phys*., **30**, 120 (1959).
7. E.M. Chudnovsky and L. Gunther, *Phys. Rev. B*, **37**, 9455 (1988).
8. R.D. Mcmicheal, R.D. Shull, L.J. Swartzendruber, L.H. Bennett and R.E. Watson, *J. Magn. Magn. Mater.*, **111**, 29 (1992).
9. J.-H. Lee, K.-H. Chung, J.-H. Yoon, J.-E. Oh, M.-S. Kim, K.-M. Yang and S.-H. Lee, *Elast. Compos.*, **46**, 311(2011).
10. K. Chung and K. Yoon, *Elast. Compos.*, **45**, 106 (2010).
11. R. West, D. David, P.I. Djurovich, K.L. Stearly, K.S.V. Srinivasan and H. Yu, *J. Am. Chem. Soc.*, **103**, 7352 (1981).
12. R. West, D. David, P.I. Djurovich, K.L.H. Yu and R. Sinclair, *Ceram. Bull.*, **62**, 823 (1983).
13. J. Joo and C.Y. Lee, *J. Appl. Phys.*, **88**, 513 (2000).
14. D.H. Chen and X.R. He, *Mater. Res. Bull.*, **36**, 1369 (2001).
15. S. Liu, X. Wei, M. Chu, J. Peng and Y. Xu, *Colloids Surf. B*, **51**, 101 (2006).